Journal of Environmental Chemical Engineering 5 (2017) 1219–1226

Contents lists available at ScienceDirect

Journal of Environmental Chemical Engineering

journal homepage: www.elsevier.com/locate/jece

Influence of solvent in the synthesis of nano-structured ZnO by hydrothermal method and their application in solar-still

Sayed M. Saleh[a,*], Ahmed M. Soliman[b,c], Mohamed A. Sharaf[c], Vishal Kale[d], Bhushan Gadgil[e]

[a] Chemistry Branch, Department of Science and Mathematics, Faculty of Petroleum and Mining Engineering, Suez University, 43721 Suez, Egypt
[b] Department of Engineering Sciences, Faculty of Petroleum and Mining Engineering, Suez University, 43721 Suez, Egypt
[c] Mechanical Department, Faculty of Engineering , Al Jouf University, Sakaka, KSA
[d] Department of Biotechnology, University of Turku, Tykistökatu 6A, FI-20520 Turku, Finland
[e] Turku University Centre for Materials and Surfaces (MATSURF), Laboratory of Materials Chemistry and Chemical Analysis, University of Turku, FI-20014 Turku, Finland

ARTICLE INFO

Article history:
Received 25 November 2016
Received in revised form 20 January 2017
Accepted 2 February 2017
Available online 3 February 2017

Keywords:
ZnO
Nanoparticles
Hydrothermal method
Solvent effect
Solar still

ABSTRACT

This article presents a novel work related to synthesis and utilize ZnO nanoparticles to enhance solar still distillation productivity. The hydrothermal synthesis method based on using different solvents such as methanol and ethylene glycol was used in the synthesis of ZnO nanoparticles. The resulting oxide nanomaterials nano-rod (100 nm length, 10–15 nm diameter) and nano-sphere (250 nm diameter) were characterized using field emission scanning electron microscope (FESEM), transmission electron microscope (TEM), UV–vis absorption spectroscopy, and X-ray diffraction. The analyses show that the solvent controlled the size and morphology of the produced nano-particles. The synthesized ZnO nonmaterial is used as an important application for solar still. The effect of ZnO nonmaterial shape and its concentration on the performance of the solar still were investigated. The results showed a great effect of the nanomaterials on the performance of the solar still. Results reveal that nano-rod shape achieves range of 30% and 38% of increase in solar still productivity and efficiency respectively compared against the nano-sphere shape.

1. Introduction

Nanostructured materials have attracted extensive attention due to their valuable physical and chemical properties which fluctuate strongly from their bulk material and prospective applications in numerous nano-optical [1–4] or nano-electric devices [5]. Recently, scientists have utilized numerous techniques to synthesize different types of inorganic oxide nanomaterials for using in a broad range of important applications, in particular their applications in drug delivery and biosensors technology [6], gas sensor [7], catalysis and coating [8,9]. Moreover, numerous researches introduce plentiful methods that monitor size and morphology of metal oxide nanomaterials. Thus; the distinct shapes of the one dimensional nanoparticles extremely exhibit different physical, mechanical, electrical and optical properties [10–12]. Furthermore; the more intricate structures, two or three dimensional structures, of these oxide micro or nanomaterials such as nanowire, nanospheres, and nanoplates are present distinctive properties [13–15].

Zinc oxide (ZnO) is considered the most essential semi-conductors that utilizing in immense scientific applications, this inorganic oxide material has a direct band gap of 3.37 eV and a large excitation binding energy of 60 meV [16]. According to their unique properties, zinc oxide has been established to have tremendous applications in optical, mechanical, electrical, electrochemical devices [17] include solar cells [18], Ultra Violet (UV) laser [19], laser diode [20], and highly performance nanostructure sensors [21]. Numerous methods based chemical and physical have been developed for synthesizing large numbers of metal oxide nanomaterials in short period of time. The most frequently methods comprise sol-gel technique [22], electrochemical [23], hydrothermal and chemical precipitation [24].

ZnO is a biocompatible material, non-noxious, and inexpensive, which commonly used as semiconductor in dye degradation. Due

* Corresponding author.
E-mail address: sayed.saleh@suezuniv.edu.eg (S.M. Saleh).

http://dx.doi.org/10.1016/j.jece.2017.02.004
2213-3437/

to its photocatalytic activities in the presence of UV light, zinc oxide nanomaterials can be used efficiently to dye decolorization and detoxification from waste water [25]. These nanomaterials were utilized to remove azo-dyes [26] and pesticide [27] from contaminated water. There are several physical and chemical properties of ZnO nanomaterials depend strongly on the mechanism of their crystal structure growth, and it has proven that control of surface morphology and crystal structure could be enhanced their photocatalytic activity [28]. Therefore, significant efforts have been dedicated in order to develop efficient methods for synthesizing ZnO nanomaterials with different size and surface morphology.

The solar still is one of the most cost effective methods for obtaining fresh water which may share the solving plan of water shortage [29–31]. One of the major problems for the whole world, and in particular, in the third world is the availability of pure, clean and healthy water, especially in remote areas. Desalination systems using traditional fuels have been used in many countries in the Middle and Near East to produce fresh water. The performance of solar distillation systems depends on climatic parameters, e.g. ambient temperature, solar radiation intensity and weather conditions, design parameters, e.g. inclination angle, and operational parameters, such as orientation of the solar still and the brine water depth [32]. It has been found that with the increment in solar radiation intensity [33] and ambient temperature, the productivity of the solar still increases [34]. For Middle Eastern countries, solar radiation is very high and almost always available, which would make the deserts a good location for solar plants. Using solar energy systems in desalinating plants is obviously practical and good for the environment.

Recently, researches have shown that the utilization of different nanofluids can improve the efficiency of salt water desalination process [35–38]. However, some problems exist and affect the solar still productivity as the nanoflid are practically in direct contact with salt water. In comparison to these previous works, the authors present a very simple route of utilizing nanoparticles in solar still, because the basin is brushed using special paint containing nanomaterial that does not add to the saline water. Moreover, the novelty of this work not only to produce a new different types of zinc oxide nanoparticles based hydrothermal method but also investigates the effect of these nanoparticles on the productivity and the efficiency of solar still.

In this work, we report the synthesis of hierarchical ZnO nanostructure via different solvent assisted hydrothermal method and their application as a photocatalyst. The effect of solvent on morphology of ZnO has also been studied. It is found that solvent plays an important role in the formation and self assembly of ZnO architectures. Morphology and concentration factors were applied to investigate its effect on solar still productivity and efficiency as figures of merit. One advantage includes this application that nanomaterials weren't in direct contact with the saline water. However; ZnO nanomateriales painted over the solar still basin. The effect of solar radiation, ambient temperature, and different operating conditions is also considered. Eventually, new equation was created in order to realize the effect of the nanomaterials concentration on efficiency and productivity of the solar still.

2. Material and methods

2.1. Materials

All reagents, including zinc nitrate ($Zn(NO_3)_2{\cdot}6H_2O$), Potassium hydroxide (KOH), methanol, ethylene glycol and hexadecyltrimethyl ammonium bromide (CTAB), these are all of analytical grade chemicals produced from Sigma Aldrich and were used as received.

2.2. Instruments

Transmission electron microscopy (TEM) images were carried out by using a JEOL instrument (TEM, JEOL Inc., Tokyo, Japan) at an acceleration voltage of 200 kV. Field emission scanning electron microscopy (FESEM) was performed using Hitachi S-4800 Type II Ultra-High Resolution Field Emission Scanning Electron Microscope at 20 kV. The XRD measurements were measured using "a Philips" diffractometer (type PW 1730) with Ni–filtered, Co radiation ($\lambda = 1.79$) at 30 kV and 20 mA. The specific surface area of the synthesized particles was determined by the nitrogen adsorption method of Brunauer, Emmett, and Teller [39] utilizing Micrometrics instrument model ASAP 2010. The UV–visible recording spectrophotometer shimadzu-Japan was used to measure absorbance of light wavelengths of the solid ZnO nanomaterials.

2.3. Synthesis of ZnO nanorods

The precursor solutions were prepared in methanol. In a typical procedure, 10 mL of 1 M KOH solution was added to 50 mL of methanol under magnetic stirring, and 10 mL of 0.4 M Zn $(NO_3)_2{\cdot}6H_2O$ solution was added. The solution was stirred for 10 min then, 20 mL of the mixture was transferred into a Teflon-lined stainless steel autoclave with a capacity of 25 mL. The autoclave was sealed and kept under heating at 120 °C for 5 h. CTAB were introduced to control the morphology of the ZnO nanostructure. After the reaction was completed, the mixture was cooled at room temperature, and the white powder was separated from the solution by centrifugation and washed with hot water and ethanol. Finally, the product was kept dispersed in ethanol.

2.4. Synthesis of ZnO nanospheres

The synthetic procedure was similar to that of the ZnO nanorods except the solvent changed from methanol to ethylene glycol.

2.5. Setup and procedure

Half tubular solar still (HTSS) is manufactured and examined under the meteorological data of the location of operation. The half-tubular solar still was tested under climate conditions of Suez (latitude of 29° 966′ N, longitude of 32° 549′ E) in a typical summer month, on June 8th, 2016. Hence this site and time are the best for meteorological measurement of solar energy. Summer is the best season to choose for experiments due to high solar intensity. A schematic diagram of a half-tubular solar still with a radius of 200 mm is shown in Fig. 1(a and b) shows the thermocouples positions on the still.

The half tubular solar still model has a water basin with dimensions of $1200 \times 150 \times 30$ mm. Further; this model consists of a basin liner which absorbs incident solar radiation that is transmitted through the tubular glass cover. The basin liner is made of a galvanized steel sheet of 1 mm thickness and coated with black paint for better solar absorption. It has an area of $1.2\ m \times 0.15\ m$. Heat losses occurred from the bottom and side walls are neglected. The condensing cover of the solar still is made of highly transparent plastic of 3 mm thickness and is placed on the vertical walls of the distillate channel of the solar still. The condensed water gets collected in a distillate channel.

A plastic pipe is connected to the distillate channel to drain distillate water to a scaled measuring jar and a drainage pipe is connected to remove wastes inside the solar still. Rubber gaskets are provided between the glass cover and the vertical walls to prevent heat loss. Thermocouples shown in the schematic Fig. 1(a)

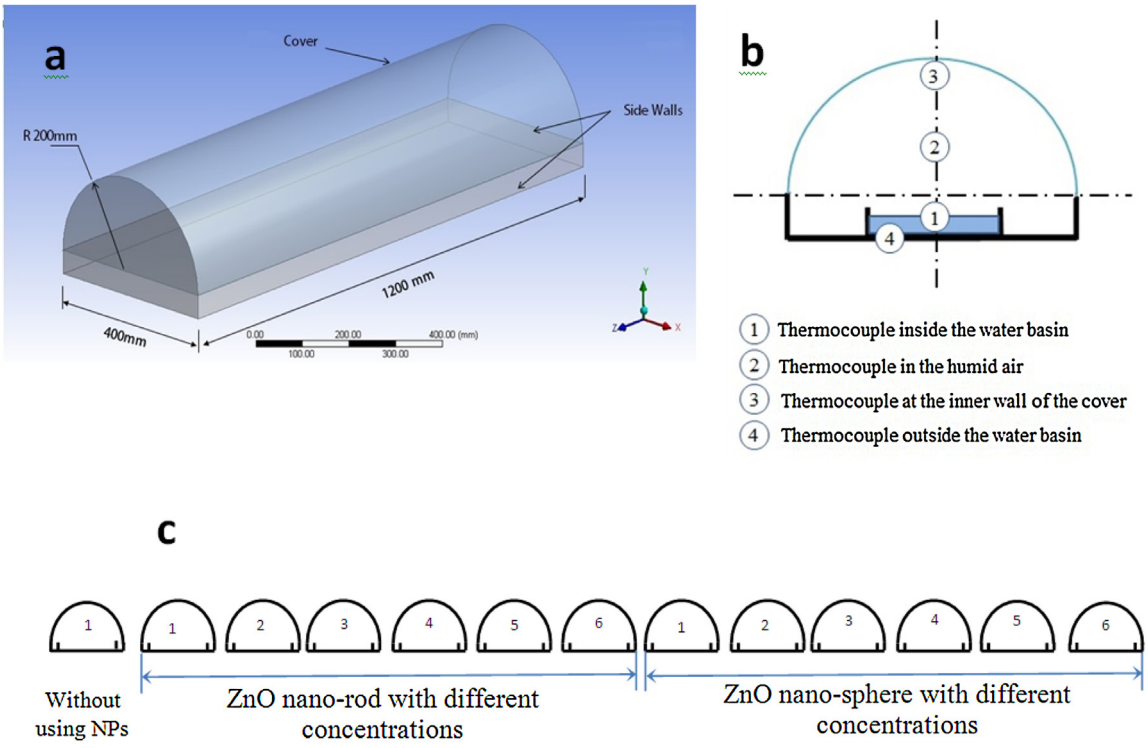

Fig. 1. (a) 3-D dimensions diagram of half-tubular solar still; (b) Schematic diagram of the half-tubular solar still with thermocouples locations; and c: arrangement of thirteen solar still.

are fixed into the solar still to measure the basin liner, as well as glass and water temperatures. The thermocouple fixed outside the basin measures the outside temperature of the basin. Thermocouples are connected to digital temperature indicators to indicate the hourly temperature readings. The basin was coated with industrial black paint only, for better solar absorption, or mixed with ZnO nanometerials. Six models were tested with different concentrations of ZnO nanomaterials for each type of the synthesized nanomaterials. The galvanized steel trays were sprayed with a mixture of ZnO nanomaterials doped paint with increasing nanomaterials concentration from zero to 600 mg.

The volume of the paint required for the surface area of the water basin was utilized to be 100 mL, which is the same volume for all models. The coating was produced with spray gun and the well painted basin, then filled the water and covered with tubular plastic cover. The solar still model works by absorbing the incident solar radiation that is transmitted through the tubular plastic cover then transferring its energy to the metal basin and to the saline water. Evaporation occur by increasing the basin temperature leaving the brine and releasing the fresh vapor. The cover would condense the vapor and accumulate the product in the tray.

3. Results and discussion

3.1. Characterization of nanomaterials

Reaction medium acts an essential role in growth mechanism of ZnO nanoparticles [40]. Memorably, above the critical micelle concentration, the aqueous solution of any surfactant is a homogeneous mixture of polar and non-polar groups. In the first stage of the synthesis process, the zinc ion precursor was first distributed between the alkali water/ethylene glycol or water/methanol and micelle CTAB phases, then chelating of the zinc ions by ethylene glycol or methanol groups take place to form high polar active complex intermediate. Further, the zinc-complexes come closer to the positively charged ammonium groups of CTAB due to the electrostatic interactions between the cationic micelles head groups and negatively charged chelating groups of zinc ions which support the zinc precursor localization on the micelle surface. Eventually, the surface of micelle is the favored active site for producing polar intermediate due to the excessive micelle polarity. It was found that CTAB inhibits the aggregation of the formed nanomaterials besides it has an effect on nucleation and growth processes of crystallites during synthesis [41].

Two different morphologies of ZnO nanostructures were obtained using different solvents. The different synthesized nanoparticles were characterized in terms of size and morphology utilizing FE-SEM. The morphology of ZnO nanorods synthesized using methanol is compared with that of ZnO nanospheres prepared using ethylene glycol. Fig. 2(a) shows characteristic FE-SEM images of the synthesized ZnO rods. The rods are transparent with a length of around 100 nm and diameter of around 10–15 nm. The higher surface area of these particles in comparison to nanospheres could be attributed to these obvious data. Most of the rods have a smooth side faces. On the other hand, an individual sphere like ZnO nanostructure with the diameter of 250 nm is observed from the magnified FE-SEM image shown in Fig. 2(b). The observation of rough surface is due to the crystal of ZnO, whose self-assembly growth expresses regular morphology.

The powder X-ray diffraction (XRD) patterns were recorded in the 2θ range of 20−80° with a scanning step of 0.01°. Fig. 3 shows the XRD patterns of the two products obtained in different solvent. All the diffraction peaks are in agreement with the JCPDS file of ZnO, which can be indexed as a hexagonal phase of ZnO. No peaks attributable to possible impurities are observed. The sharp diffraction peaks manifested that the as prepared ZnO nanostructures have high crystallinity. The strongest peaks correspond to the planes (100), (002), (101), (102), (110), (103), (200), (112) and (201), in both cases planes corresponding to of hexagonal wurtzite ZnO are clearly observed [42]. The TEM data indicate the high

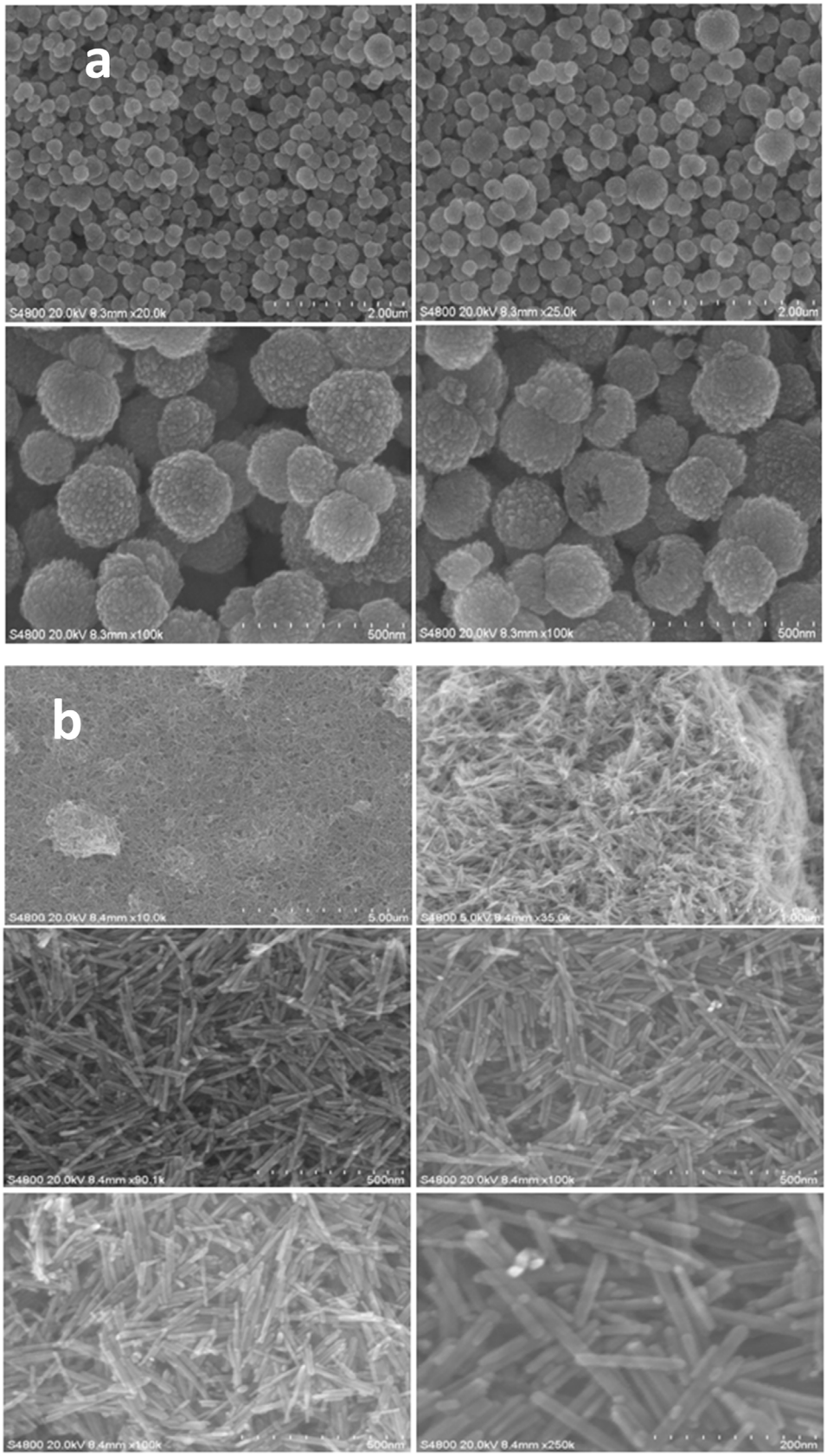

Fig. 2. (a). FE-SEM images of samples obtained using Methanol; (b) samples obtained using EG.

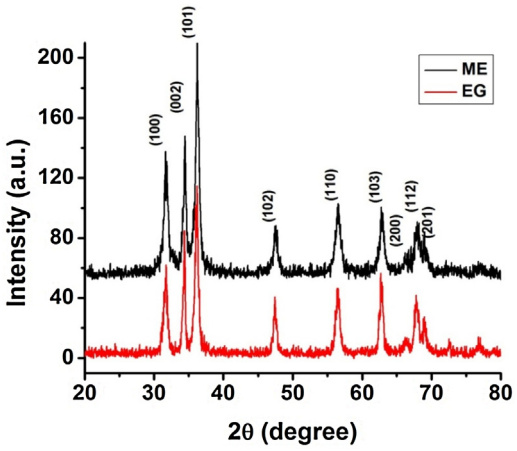

Fig. 3. The XRD pattern of the ZnO powder using methanol and EG.

solvent effect on the synthesis process of the ZnO nanoparticles. The Cu signal is attributed to the copper meshes for TEM Fig. 4(a) is a typical TEM image of ZnO nanorods. The nanorods are straight and smooth with 100 nm length and 10–15 nm diameter.

The optical properties of various shapes of ZnO nanostructures were studied. As shown in Fig. 4(b), ZnO nanostructure with various shapes display different profiles of UV–vis absorption spectra, especially for nanorods and nanospheres. The absorption of the ZnO nanospheres synthesized in ethylene glycol shows sharp edge at ~377 nm, and the absorption of the ZnO nanorods prepared in methanol shows absorption edge at ~392 nm, the red shift in the UV spectrum is related to its band edge absorption, since the direct band gap (E_g) of the ZnO material were calculated from the absorbance values 3.34 and 3.22 for nano-sphere and nano-rod particles respectively [43]. Moreover, the specific surface area (SN_2) of the two types of ZnO nanoparicles was measured by BET measurements according to Brunauer, Emmett, and Teller [39]. The SN_2 was determined to be 88.512 and 151.869 $m^2 g^{-1}$ for spherical and rod nanoparticles respectively.

The production of the distilled water that is produced from solar still was studied and a definite mathematical equation was

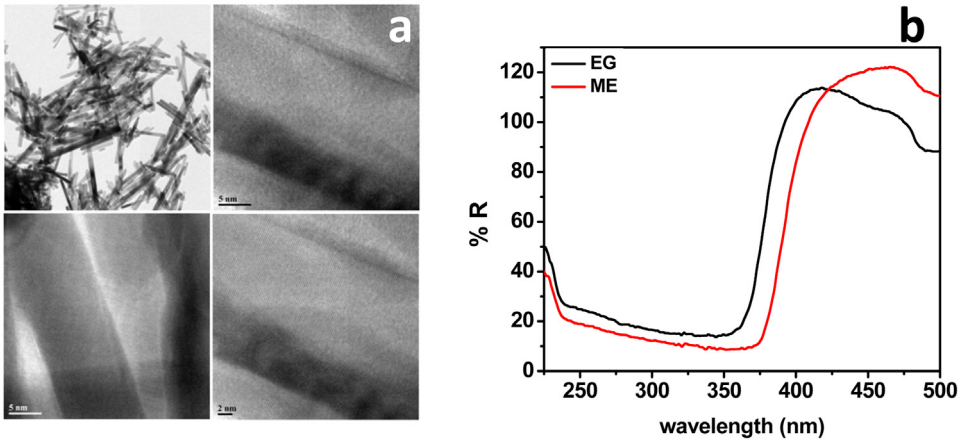

Fig. 4. (a) TEM images of ZnO sample synthesized using methanol as solvent; (b) UV–vis spectra for both ZnO nanorods and ZnO nanospheres.

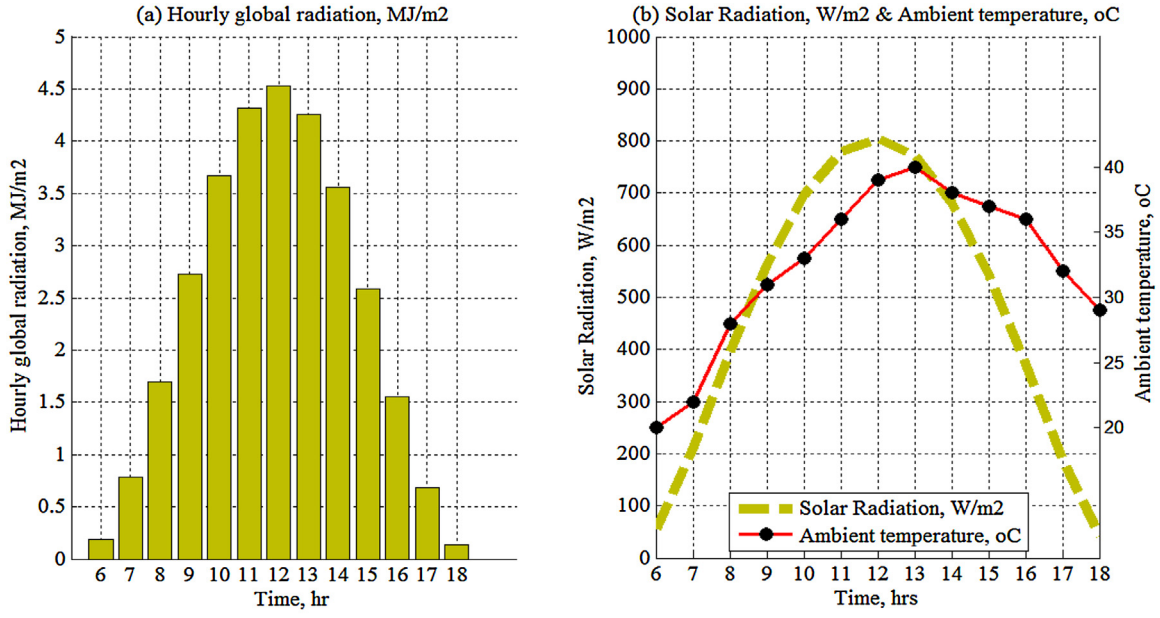

Fig. 5. The recorded data in 8th of June 2016; (a) Hourly solar radiation, W/m^2 and (b) Ambient temperature, °C vrsus time.

stated. Fig. 5 gives complete statistical and graphical information about the solar still production using ZnO nanomaterials. The production of the solar still is not only directly proportional to the temperature of the solar still but also to the concentration of the synthesized ZnO nanomaterials. Also, the accumulative production as a function of time and concentration of the synthesized ZnO nanomaterials is represented by the 3D graph. This shows that the accumulative productivity increases with time and concentration of the nanomaterials. In addition, after the ZnO nanomaterials concentration reaches an approximate definite limit per 100 mL of the liquid paint the accumulative productivity becomes constant.

3.2. Solar still results

Fig. 5 shows the daily measurements of the weather conditions for solar intensity and ambient temperature were taken from the 1st up to the 8th of June 2016, from 09:00 am to 06:00 pm. It is obvious from Fig. 5 that the radiation maximum value achieves about 750–800 W/m^2 which considered high and optimum for the distiller operation. Furthermore; the ambient temperature is also high meaning by this reducing the heat losses from the still to the ambient at discarded levels.

Fig. 6(a) shows the effect of two shapes (Nano-rod & Nano-sphere) of concentration on accumulative productivity, kg/m^2 and the basin water temperature, °C for half tubular solar still (HTSS). For both shapes in Fig. 6(a and b), increasing the concentration percentages would increase the productivity and the temperature. Moreover; the maximum values are recorded at the middle of the day according to the effect of higher rates of solar radiation. Generally, Nano-rod shape recorded the higher results compared against the Nano-spherical due to some reasons such as surface area [44], particle geometry and the density of the molecules per unit area [45]. Fig. 6(c) shows that the productivity reaches about 4.2 kg/m^2 vs. 3 kg/m^2 for rod shape at concentrations 300–400 mg. It is estimated that the percentage of increasing of the productivity due to the concentration effect from 100 mg to 400 mg is about 30%. The temperature profile in Fig. 6(b) is massively affected by the solar radiation sine curve. At the same time, the increasing of the concentration would also increase the temperature levels of the still basin. For the basin temperature, the percentage of increasing reaches about 25% at middle of the day due to the effect of concentration combined with the natural increase of the solar radiation. Eventually, the nano-rod shape recorded higher results than the nano-sphere shape due to the surface area of the particles. The efficiency of solar still η is calculated from the following relation:

$$\eta = \frac{q_{ev}}{H} = \frac{m_{ev}L}{H}$$

Where: q_{ev} is the heat of evaporation, kWh, m_{ev} is the mass of evaporated vapor (daily distilled water, kg), H is the total solar radiation fall upon the still surface, kWh, L is the latent heat of evaporation, kJ/kg.

Fig. 7 shows the effect of concentration of the two shapes on the efficiency of solar stills. It is obvious form the figure that nano-rod achieves higher results than the spherical one. At maximum levels of concentration between 300 and 400 mg, the percentage of increase of the still efficiency reaches about 38%. These results could be attributed to the increment of the surface area per unit volume of the nano-rod nanomaterials with respect to the spherical one. Furthermore, the approximated value of the surface area of the rod-shape per unit volume for each particle (100 nm length, 10–15 nm diameter) is higher than that of the spherical nanomaterials (250 nm diameter) [46]. Also, the rods have a smooth side faces could be increase the homogeneity and dispersity of the nanomaterials on the surface of the still basin.

4. Conclusion

Half tubular solar still is manufactured and used to desalinate seawater by the aid of nanomaterials. The aim is to enhance the solar still productivity by adding the nanomaterials to the still basin paint. It has been shown that the prospective for alteration size and shape of ZnO nanoparticles. The nanoparticles were synthesized by hydrothermal process varying the solvent type from methanol to ethylene glycol under the same reaction conditions. With this synthesis procedure, it was feasible to produce small particles with a very high symmetry at comparatively low temperatures. The shape of the ZnO nanomaterials was completely different from nanorods in case of using methanol as solvent to spare in case of ethylene glycol. Moreover, in comparison between the present results with the literature gives a proof that it is not only the synthesis conditions (temperature, types of ions, concentration, acidity of the medium, surfactant) but also the solvent plays an important role in controlling the ZnO nanomaterials shape and structures. As an important application, the

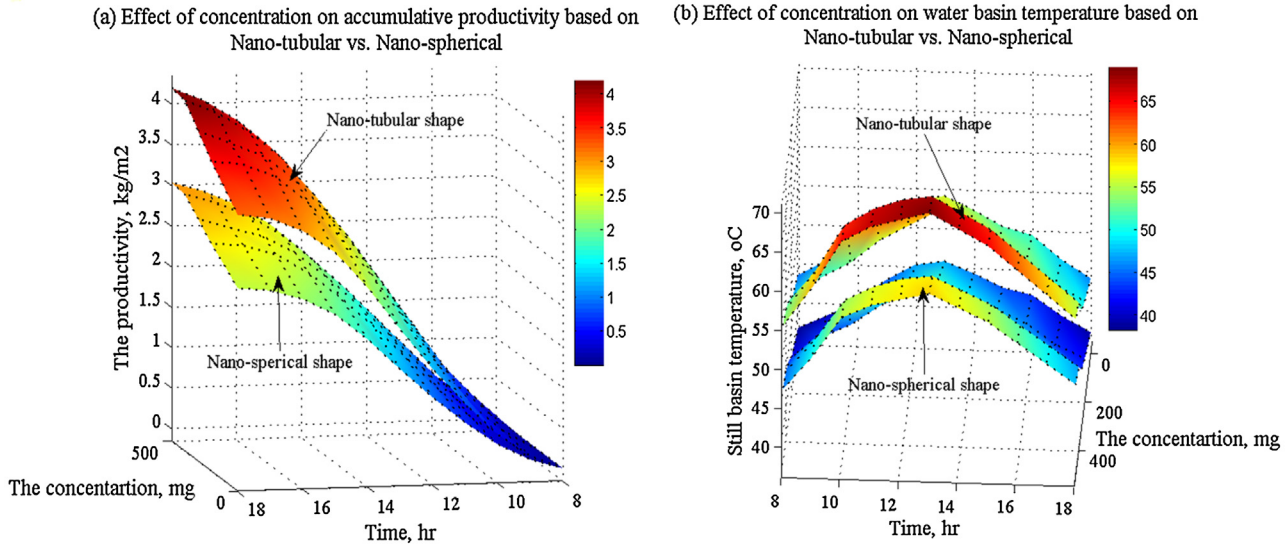

Fig. 6. (a) The effect of concentration on accumulative productivity, kg/m^2; (b) the basin water temperature, °C at different shapes of nanomaterials.

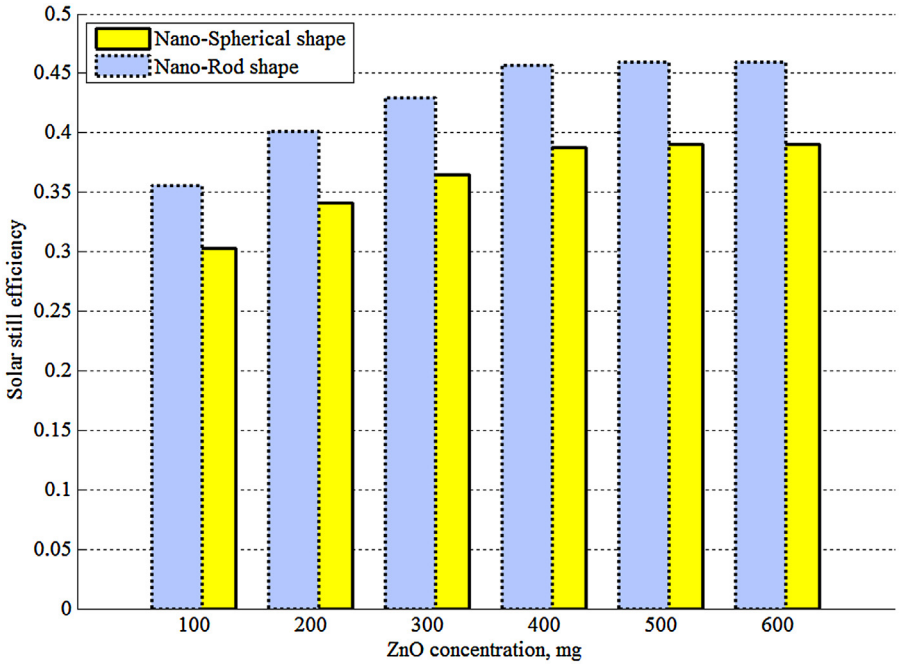

Fig. 7. The concentration effect of different types of nanomaterials on the daily efficiency.

synthesized sphere ZnO nanoparticles were used in solar still. Different concentrations of the nanomaterials were mixed with black.

The concentration range of nanomaterials was varying from zero to approximately 600 mg per 100 mL of the liquid paint. It was found that the efficiency and accumulative productivity of the solar still increases directly with increasing the amount of the sphere ZnO nanomaterials within range from 0 to 600 mg per 100 mL of the paint. Moreover; two shapes of nanoparticles (rod and sphere) were used. Results show that the efficiency and the productivity of the solar still increase by 38% and 30% respectively in case of using the nano-rod shape. The high performance of the solar still in case of utilizing nano-rod could be attributed to the smooth surface geometry and high surface area of the rod-shape nanomaterials.

References

[1] M.J. Zheng, L.D. Zhang, G.H. Li, W.Z. Shen, Fabrication and optical properties of large-scale uniform zinc oxide nanowire arrays by one-step electrochemical deposition technique, Chem. Phys. Lett. 363 (2002) 123–128.
[2] O. Amiri, M. Salavati-Niasari, A. Rafiei, M. Farangi, 147% improved efficiency of dye synthesized solar cells by using CdS QDs, Au nanorods and Au nanoparticles, RSC Adv. 4 (107) (2014) 62356–62361.
[3] M. Sabet, M. Salavati-Niasari, O. Amiri, Using different chemical methods for deposition of CdS on TiO_2 surface and investigation of their influences on the dye-sensitized solar cell performance, Electrochim. Acta 117 (2014) 504–520.
[4] O. Amiri, M. Salavati-Niasari, M. Sabet, Davood Ghanbari, Synthesis and characterization of CuInS 2 microsphere under controlled reaction conditions and its application in low-cost solar cells, Mater. Sci. Semiconduct. Proc. 16 (6) (2013) 1485–1494.
[5] M.H. Sun, Q.F. Zhang, J.L. Wu, Electrical and electroluminescence properties of As-doped p-type ZnO nanorod arrays, J. Phys. D: Appl. Phys. 40 (2007) 3798–3802.
[6] T.Y. Liu, H.C. Liao, C.C. Lin, S.H. Hu, S.Y. Chen, Biofunctional ZnO nanorod arrays grown on flexible substrates, Langmuir 22 (2006) 5804–5809.
[7] J.X. Wang, X.W. Sun, Y. Yang, H. Huang, Y.C. Lee, O.K. Tan, L. Vayssieres, Hydrothermally grown oriented ZnO nanorod arrays for gas sensing applications, Nanotechnology 17 (2006) 4995–4998.
[8] T. Sakano, Y. Tanaka, R. Nishimura, N.N. Nedyalkov, P.A. Atanasov, T. Saiki, M. Obara, Surface enhanced Raman scattering properties using Au-coated ZnO nanorods grown by two-step, off-axis pulsed laser deposition, J. Phys. D: Appl. Phys. 41 (2008) 235304.
[9] R. Shi, P. Yang, X. Song, J. Wang, Q. Che, A. Zhang, ZnO flower: self-assembly growth from nanosheets with exposed {1-100}facet, white emission, and enhanced photocatalysis, Appl. Surf. Sci. 366 (2016) 506–513.
[10] P. Nuengmatcha, S. Chanthai, R. Mahachai, W. Oh, Visible light-driven photocatalytic degradation of rhodamine B and industrial dyes (texbrite BAC-L and texbrite NFW-L) by ZnO-graphene-TiO_2 composite, J. Environ. Chem. Eng. 4 (2016) 2170–2177.
[11] S.J. Jeong, H.S. Moon, J. Shin, B.H. Kim, D.O. Shin, J.Y. Kim, Y.H. Lee, J.U. Kim, S.O. Kim, One-dimensional metal nanowire assembly via block copolymer soft graphoepitaxy, Nano Lett. 10 (2010) 3500–3505.
[12] G.D. Yuan, W.J. Zhang, J.S. Jie, X. Fan, J.X. Tang, I. Shafiq, Z.Z. Ye, C.S. Lee, S.T. Lee, Tunable n-type conductivity and transport properties of Ga-doped ZnO nanowire arrays, Adv. Mater. 20 (2008) 168–173.
[13] J. Qin, X. Zhang, C. Yang, M. Cao, M. Ma, R. Li, ZnO microspheres-reduced grapheme oxide nanocomposite for photocatalytic degradation of methylene blue dye, Appl. Surf. Sci. 392 (2017) 196–203.
[14] C. Lei, M. Pi, C. Jiang, B. Cheng, J. Yu, Synthesis of hierarchical porous zinc oxide (ZnO) microspheres with highly efficient adsorption of Congo red, J. Colloid Interface Sci. 490 (2017) 242–251.
[15] B. Weintraub, Y.G. Wei, Z.L. Wang, Optical fiber/nanowire hybrid structures for efficient three-dimensional dye-sensitized solar cells, Angew. Chem. Int. Ed. 48 (2009) 8981–8985.
[16] U. Ozgur, Y.I. Alivov, C. Liu, A. Teke, M.A. Reshchikov, S. Dogan, V. Avrutin, S.J. Cho, H. Morkoc, A comprehensive review of ZnO materials and devices, J. Appl. Phys. 98 (2005) 041301.
[17] S.C. Pillai, J.M. Kelly, R. Ramesh, D.E. McCormack, Advances in the synthesis of ZnO nanomaterials for varistor devices, J. Mater. Chem. C 1 (2013) 3268–3281.
[18] C.K. Xu, P. Shin, L.L. Cao, D. Gao, Preferential growth of long ZnO nanowire array and its application in dye sensitized solar cells, J. Phys. Chem. C 114 (2010) 125–129.
[19] M.H. Huang, S. Mao, H. Feick, H. Yan, Y. Wu, H. Kind, E. Weber, R. Russo, P. Yang, Room-temperature ultraviolet nanowire nanolasers, Science 292 (2001) 1897–1899.
[20] F. Claeyssens, A. Klini, A. Mourka, C. Fotakis, Laser patterning of Zn for ZnO nanostructure growth: comparison between laser induced forward transfer in air and in vacuum, Thin Solid Films 515 (2007) 8529–8533.
[21] J. Zhou, Y.D. Gu, Y.F. Hu, W.J. Mai, P.H. Yeh, G. Bao, A.K. Sood, D.L. Polla, Z.L. Wang, Gigantic enhancement in response and reset time of ZnO UV nanosensor by utilizing Schottky contact and surface functionalization, Appl. Phys. Lett. 94 (2009) 191103.
[22] S.J. Kwon, J.H. Park, J.G. Park, Patterned growth of ZnO nanorods by micromolding of sol–gel-derived seed layer, Appl. Phys. Lett. 87 (2005) 133112.
[23] M. Shohel, M.S. Miran, M.A.B.H. Susan, M.Y.A. Mollah, Calcination temperature-dependent morphology of photocatalytic ZnO nanoparticles prepared by an electrochemical–thermal method, Res. Chem. Intermed. (2015) 1–17.
[24] N.U. Sangari, C.S. Devi, Synthesis and characterization of nano ZnO rods via microwave assisted chemical precipitation method, J. Solid State Chem. 197 (2013) 483–488.

[25] S.M. Lam, J.C. Sin, A.Z. Abdullah, A.R. Mohamed, Photocatalytic degradation of resorcinol, an endocrine disrupter, by TiO_2 and ZnO suspensions, Environ. Technol. 34 (9–12) (2013) 1097–1106.
[26] K. Milenova, I. Avramova, A. Eliyas, V. Blaskov, I. Stambolova, N. Kassabova, Application of activated M/ZnO M = Mn, Co, Ni, Cu, Ag in photocatalytic degradation of diazo textile coloring dye, Environ. Sci. Pollut. Res. Int. 21 (21) (2014) 12249–12256.
[27] E. Topkaya, M. Konyar, H.C. Yatmaz, K. Ozturk, Pure ZnO and composite ZnO/TiO_2 catalyst plates: a comparative study for the degradation of azo dye, pesticide and antibiotic in aqueous solutions, J. Colloid Interface Sci. 430 (2014) 6–11.
[28] Y. Yang, Y. Li, L. Zhu, H. He, L. Hu, J. Huang, F. Hu, B. He, Z. Ye, Shape control of colloidal Mn doped ZnO nanocrystals and their visible light photocatalytic properties, Nanoscale 5 (21) (2013) 10461–10471.
[29] Human Development Report 2006 UNDP, 2006, Coping with water scarcity Challenge of the twenty-first century UN-Water, FAO, 2007.
[30] B.A. Jubran, M.I. Ahmed, A.F. Ismail, Y.A. Abakar, Numerical modelling of a multi- stage solar still, Energy Convers. Manag. 41 (2000) 11071–11214.
[31] K. Sampathkumar, T.V. Arjunan, P. Pitchandi, P. Senthilkumar, Active solar distillation-A detailed review, Renew. Sustain. Energy Rev. 14 (2010) 1503–1526.
[32] G.N. Tiwari, A. Tiwari, Solar Distillation Practice for Water Desalination Systems, Anamaya, New Delhi, 2007.
[33] H.P. Garg, H.S. Mann, Effect of climatic, operational and design parameters on the year round of single-sloped and double-sloped solar still under Indian arid zone conditions, Sol. Energy 18 (1976) 159–163.
[34] J.A. Eibling, S.G. Talbert, G.O.G. Lof, Solar stills for community use-digest of technology, Sol. Energy 13 (1971) 263–276.
[35] L. Sahota, G.N. Tiwari, Effect of Al_2O_3 nanoparticles on the performance of passive double slope solar still, Sol. Energy 130 (2016) 260–272.
[36] L. Sahota, G.N. Tiwari, Effect of nanofluids on the performance of passive double slope solar still: a comparative study using characteristic curve, Desalination 388 (2016) 9–21.
[37] Z.M. Omara, A.E. Kabeel, F.A. Essa, Effect of using nanofluids and providing vacuum on the yield of corrugated wick solar still, Energy Convers. Manag. 103 (2015) 965–972.
[38] S.W. Sharshir, G. Peng, Lirong Wu, Nuo Yang, F.A. Essa, Showgi I.T. Mohamed, A. E. Kabeel, Enhancing the solar still performance using nanofluids and glass cover cooling: experimental study, Appl. Therm. Eng. 113 (2017) 684–693.
[39] M. Kruk, M. Jaronie, Adsorption characterization of ordered organic-Inorganic nanocomposite materials, Chem. Mater. 13 (2001) 3169–3183.
[40] J.K. Salem, T.M. Hammad, The effect of surfactants on the particle size and optical properties of precipitated ZnO nanoparticles, J. Mater. Sci. Eng. 3 (2009) 12.
[41] A. Kołodziejczak-Radzimska, T. Jesionowski, Zinc oxide-from synthesis to application: a review, Materials 7 (2014) 2811–2833.
[42] G. Ning, X. Zhao, J. Li, C. Zhang, Hugely enhanced electroluminescence from mesoporous ZnO particles, Opt. Mater. 28 (2006) 385–390.
[43] D. Chandra, S. Mridha, D. Basak, A. Bhaumik, Template directed synthesis of mesoporous ZnO having high porosity and enhanced optoelectronic properties, Chem. Commun. 17 (2009) 2384–2386.
[44] X. Zhang, J. Qin, Y. Xue, P. Yu, B. Zhang, L. Wang, R. Liu, Effect of aspect ratio and surface defects on the photocatalytic activity of ZnO nanorods, Sci. Rep. 4 (2014).
[45] M. Guo, P. Diao, X. Wang, S. Cai, The effect of hydrothermal growth temperature on preparation and photoelectrochemical performance of ZnO nanorod array films, J. Solid State Chem. 178 (10) (2005) 3210–3215.
[46] E.S. Jang, J.H. Won, S.J. Hwang, J.H. Choy, Fine tuning of the face orientation of ZnO crystals to optimize their photocatalytic activity, Adv. Mater. 18 (2006) 3309–3312.